FAILURE OF PULTRUDED GRP ANGLE-LEG JUNCTIONS IN TENSION

G.J. Turvey* and P. Wang**
* Engineering Department, Lancaster University, Bailrigg, Lancaster, LA1 4YR, UK
g.turvey@lancaster.ac.uk
** Schlumberger, Stonehouse Technology Centre, Brunel Way, Stroudwater Business Park, Stonehouse, Gloucester, GL10 3SX, UK
pwang4@stonehouse.oilfield.slb.com

ABSTRACT

Junction tensile strengths and failure modes have been determined from a series of thirty-two tension tests on two sizes of pultruded GRP (Glass Reinforced Plastic) angle profile, namely 76 x 6.4mm and 76 x 9.5mm equal-leg angles. The average ultimate tensile strengths of the angle-leg junctions of the thinner angle profiles were found to be very variable with strengths varying by 78% and 30% for the 40mm and 60mm long angle specimens respectively depending on which leg was subjected to tension. On the other hand, the average ultimate tensile strengths of the of the angle-leg junctions of the thicker 40mm and 60mm long angle specimens were much more consistent with the specimens' strengths varying by between 7% and 3% respectively. It is concluded that the large variations in junction strengths of the thinner angle specimens are most probably due to non-uniformity (wrinkling) of the fibre architecture around the junction, which is much less evident in the thicker angle specimens.

Keywords: Angles, failure, GRP, junctions, pultrusions, tensile strength

INTRODUCTION

The use of pultruded GRP (Glass Reinforced Plastic) profiles is increasing year-on-year as structural engineers become ever more proficient at combining and exploiting their advantageous characteristics, especially their high strength, low self-weight and high corrosion resistance, in a wide variety of secondary and primary infrastructure applications such as footbridges and highway bridge decks. Notable UK examples of such primary structural applications are: the Mount Pleasant Bridge over the M6 motorway and the Bonds Mill Lift Bridge over the Stroudwater canal.

The increasing use of pultruded profiles has also been stimulated by developments in knowledge and understanding of their structural behaviour which have taken place over the past two decades. In particular, US and European researchers have made major contributions through the successful completion of a wide range of analytical, numerical and experimental investigations of the elastic flexural and buckling behaviour of pultruded GRP beams and columns and the stiffness and strength of bolted/bonded joints – the building blocks of all manner of GRP structures.

At the present time, the design of pultruded structures is generally governed by stiffness criteria, i.e. deformation limits and critical buckling stresses. Only rarely is ultimate strength an issue. However, this situation may not be expected to persist over the longer term, especially as materials improve and the use of pultruded profiles in primary load-bearing structures increases.

Unsurprisingly, knowledge of the collapse behaviour of pultruded GRP beam and column profiles is presently somewhat scant. A few failure tests on WF (Wide Flange) beams have shown that collapse is triggered by separation of the compression flange from the web [1, 2]. Ultimate load tests on short WF columns [3] have shown that similar tearing of the flanges from the web precipitates collapse. Thus, it appears that characterisation of the ultimate strengths of the web-flange junctions of pultruded GRP profiles is the key to the development of greater knowledge and understanding of their collapse behaviour.

Recognition of this fact prompted the first author and his co-investigators to undertake a number of research investigations aimed at quantifying the strength properties of web-flange junctions in pultruded GRP WF profiles. Initially, research was directed at quantifying the tensile [4], shear [5] and flexural [6, 7] strengths of the junctions. In a more recent investigation, the *opening mode* flexural strength of a 102 x 6.4mm equal-leg angle profile was quantified by means of physical testing in a special-purpose test fixture [8]. This latter investigation was prompted by failure modes observed in pultruded GRP equal-leg angle profiles subjected to longitudinal compression applied through one leg.

Angle profiles are frequently used as cleats in bonded and/or bolted joints. In such situations tensile loads may be applied transverse to, rather than along, the leg(s) of the angle. The strength of the angle may then be dominated either by the transverse strength of the leg or the junction between the legs, i.e. the two parts of the angle may have different strengths. Thus, this investigation is concerned with the quantification of the load capacity of the angle-leg junction when one leg is subjected to transverse tension and the other is restrained.

ANGLE SECTION DETAILS AND TEST ARRANGEMENT

Angle Test Specimens – Geometry, Lay-Up and Material Properties

The sections investigated were Strongwell's EXTREN® 500 Series 76 x 6.4 mm and 76 x 9.5 mm equal-leg angles [Note: Reference to a trade name does not imply endorsement of the product]. The lay-ups of the angles comprise two roving layers sandwiched between three CFM layers. Polyester resin and filler constitute the matrix material. Minimum values of the longitudinal and transverse tensile elastic moduli and strengths of the angle profiles, taken from the manufacturer's design manual [9], are given in Table 1. Also included in this table are corresponding average longitudinal values obtained from tension tests on six coupons cut out of the legs of each of the two sizes of angle profile. The coupons were 300mm long and 25mm wide. They were tested without end tabs using 75mm grip lengths. It is evident that the values obtained from the coupon tests are significantly larger than the manufacturer's minimum values – 30% to 60% higher for strength and 28% to 44% higher for modulus. However, it should be recognised that it is the transverse strength values which are particularly

relevant to the present study. Unfortunately, it was not possible to conduct *meaningful* tension tests on transverse coupons because the leg lengths of the angles were too small.

The test specimens were cut out of 6 m lengths of the two sizes of angle profile, the legs of which were identified as "A" and "B". The nominal lengths of the specimens were 40 mm and 60 mm. In order to reduce variability between specimens, all of the 40 mm long specimens were cut consecutively out of the profiles before cutting out the 60 mm long specimens. The legs of each specimen were then identified as "A" and "B". Table 2 gives details of the test specimen numbers, their nominal lengths and the test arrangements for the 76 x 6.4mm angle specimens. A similar identification system was adopted for the 76 x 9.5mm thick angle specimens, except that there were only three nominally identical specimens for each length and test arrangement.

Table 1

Tensile modulus and strength properties of pultruded GRP angle profiles

Orientation Relative to the Direction of Pultrusion	**Tensile Modulus (kN/mm^2)**	**Tensile Strength (N/mm^2)**
Parallel	17.2[a] 24.8[b] 22.0[c]	207[a] 332[b] 272[c]
Transverse	5.52[a]	48.3[a]

Note: [a] Minimum values given the manufacturer's design handbook [9].
[b] Average of six tests on coupons cut out of the 76 x 6.4 mm angle.
[c] Average of six tests on coupons cut out of the 76 x 9.5 mm angle.

Table 2

Identification system and test arrangement for the 76 x 6.4mm angle sections

Angle Specimen Numbers	**Nominal Length (mm)**	**Test Arrangement**
a1 to a5 b1 to b5	40	Leg A clamped, Leg B in tension Leg B clamped, Leg A in tension
a1 to a5 b1 to b5	60	Leg A clamped, Leg B in tension Leg B clamped, Leg A in tension

Test Set Up and Testing Procedure

The procedure used to test the angle specimens was simple and straightforward. Half of the specimens were tested with leg A clamped by means of a 40 x 20 mm cross-section steel bar bolted to a horizontal steel base plate attached to the lower grip of the universal testing machine. The other half of the specimens had leg B clamped to the base plate. The vertical leg (B or A) was then clamped in the upper grip of the machine and a tensile load was applied at a rate of approximately 10kN/minute until failure occurred. During each test the vertical displacement was recorded by a linear displacement transducer with a 10mm travel. A schematic diagram of the test set up is shown in Figure 1(a) and a photograph of a 76 x 9.5mm angle, installed in the machine ready for testing to failure, is shown in Figure 1(b).

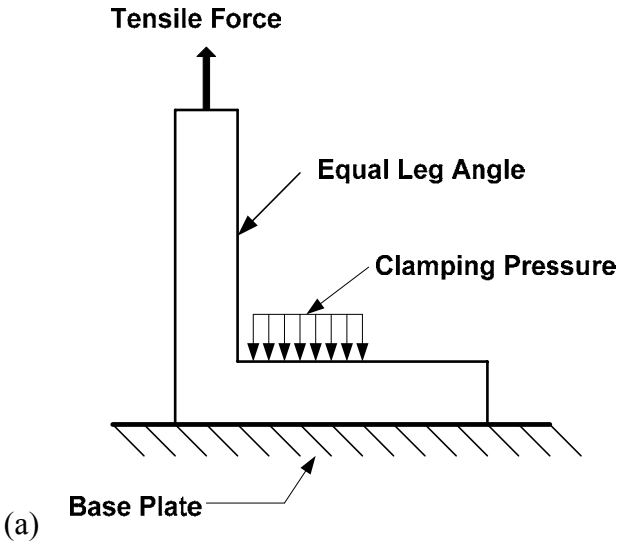

(a)

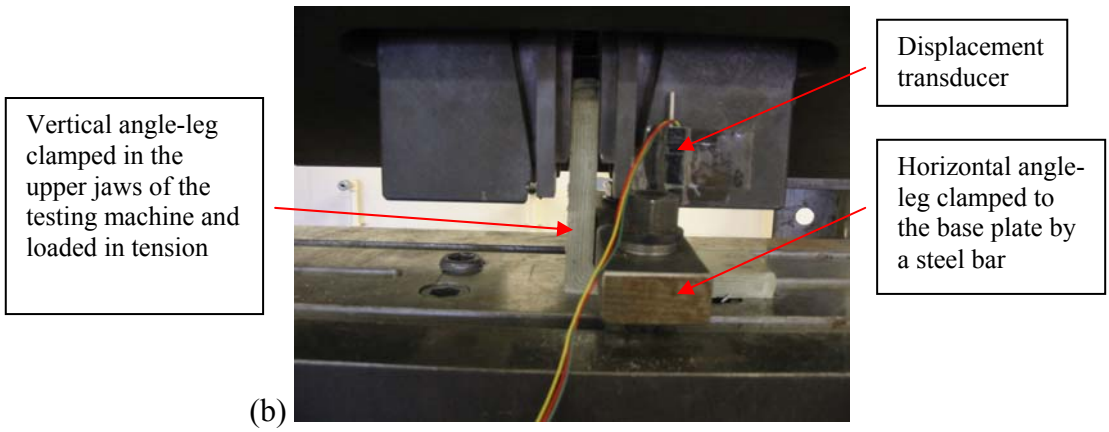

(b)

Figure 1: (a) schematic diagram of test arrangement and (b) view of an angle specimen installed in the universal testing machine ready for testing to failure.

TEST RESULTS AND DISCUSSION

Test Results for the 6.4mm Thick Angle Specimens

The load versus displacement plots obtained from two tests on 40mm long 76 x 6.4mm angle specimens are shown in Figure 2. Similar differences between the load versus displacement plots were recorded for the a2 and b2 etc 40mm long angles. However, the differences between the "a" and "b" plots of the 60mm long 76 x 6.4mm angles were somewhat less than for the 40mm long angles.

It is also evident in Figure 2 that when leg B (b1 – curve) is clamped there is a drop in load prior to reaching the ultimate load. This is consistent with the onset of significant damage (audible acoustic emission and/or visible cracks). Therefore, the peak loads immediately prior to the first load drop on the load versus displacement plots of the b1 – b5 specimens have been taken as their *damage* loads. However, when leg A is clamped (see a1 – plot) there is no evidence of a significant drop in load prior to reaching the

ultimate load and so it was not possible to identify damage loads for these specimens. Nevertheless, and in spite of the differences between the load versus displacement plots, the "a" and "b" angle specimens appear to reach their ultimate loads at roughly the same extensions, i.e. between about 1.3mm and 1.5mm.

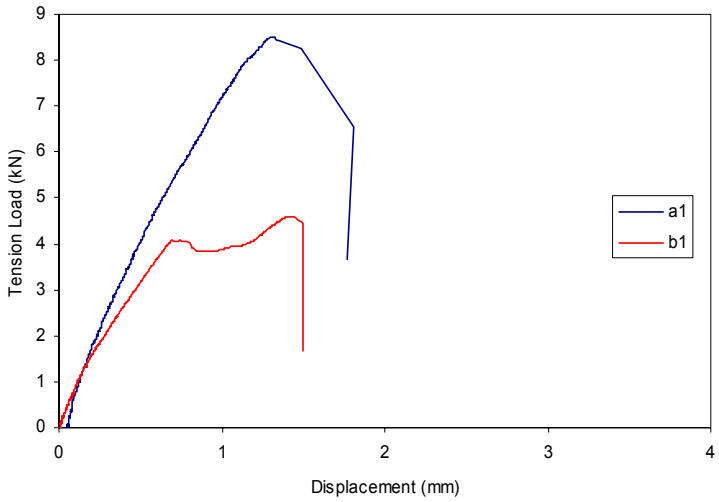

Figure 2: Comparison of load versus displacement plots of two 40mm long 76 x 6.4mm angles.

The damage and ultimate loads and loads per unit length have been determined from Figure 2 and similar plots for both the 40mm and 60mm long 76 x 6.4mm equal-leg angles. These values are given in Table 3.

From Table 3 it is clear that for both the 40mm and 60mm long 76 x 6.4mm angle specimens the *average* ultimate loads per unit length are significantly higher when leg A is clamped than when leg B is clamped. For the 40mm long specimens they are about 76% higher, whereas for the 60mm long specimens they are about 29% higher. However, the *average* damage loads per unit length do not vary much with specimen length. The value for the 40mm long angle specimens with leg B clamped is about 11% higher than that for the 60mm specimens. Again, it should be appreciated that there was no evidence of damage in the plots of the a1 – a5 specimens when leg A was clamped.

Load versus displacement plots for two 40mm long 76 x 9.5mm equal-leg angles are shown in Figure 3. It is evident that the curves are very similar in so far as there are no significant load drops prior to reaching the ultimate load. Moreover, the ultimate load of specimen b1 is only marginally lower than that of specimen a1. Furthermore, their displacements at ultimate load are similar, i.e. between about 2.2mm and 2.5mm. Hence, the load versus displacement responses depicted in Figure 3, together with the a2 – b2 etc plots indicate that the ultimate loads are much less dependent on which angle-leg (A or B) is clamped - this is particularly so for the 60mm long angle specimens.

Table 3

Damage and ultimate loads and corresponding loads and average loads per unit length of 40mm and 60mm long 76 x 6.4mm equal-leg angles

Angle Specimen Number	Actual Length (mm)	Load		Load per Unit Length		Average Load per Unit Length	
		Damage (kN)	Ultimate (kN)	Damage (N/mm)	Ultimate (N/mm)	Damage (N/mm)	Ultimate (N/mm)
Nominal Length = 40mm							
a1	39.9	---	8.50	---	213.03	---	194.76
a2	36.6	---	7.85	---	214.48		
a3	39.2	---	8.10	---	206.63		
a4	41.0	---	7.20	---	175.61		
a5	39.5	---	6.48	---	164.05		
b1	42.0	4.05	4.60	96.43	109.52	101.01	110.38
b2	40.5	4.32	4.65	106.67	114.81		
b3	39.8	4.10	4.25	103.02	106.78		
b4	40.8	3.90	4.50	95.59	110.29		
b5	39.0	4.03	4.31	103.33	110.51		
Nominal Length = 60mm							
a1	60.0	---	8.38	---	139.67	---	144.99
a2	60.5	---	9.40	---	155.37		
a3	60.0	---	8.72	---	145.33		
a4	59.4	---	9.24	---	155.56		
a5	60.0	---	7.74	---	129.00		
b1	60.0	5.26	6.38	87.67	106.33	91.16	112.14
b2	60.0	5.21	6.56	86.83	109.33		
b3	60.4	6.46	6.94	106.95	114.90		
b4	60.5	5.85	7.08	96.69	117.02		
b5	59.5	4.62	6.73	77.65	113.11		

The ultimate loads of the 76 x 9.5mm angle specimens have been determined from the peak values of the load versus deflection curves in Figure 3 and similar plots for the 40mm and 60mm long a2, b2 etc specimens. These values, together with values of ultimate load per unit length and average ultimate load per unit length obtained with leg A and leg B clamped, are given in Table 4. The latter values indicate that the average values of the ultimate load per unit length are slightly higher when leg A is clamped. For the 40mm long angle specimens they are about 5.4% higher, whereas for the 60mm long specimens they are only about 1.3% higher. These percentage differences are quite small for pultruded GRP profiles, especially as it is not unusual for material strengths derived from coupon tests to vary by as much as 10%.

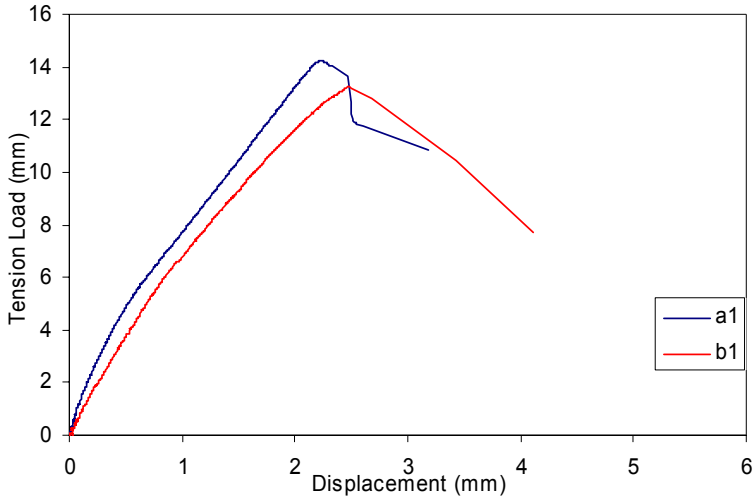

Figure 3: Comparison of load versus displacement plots of two 40mm long 76 x 9.5mm angles.

Table 4

Ultimate loads and corresponding loads per unit length for 40mm and 60mm long 76 x 9.5mm equal-leg angles

Angle Specimen Number	**Actual Length (mm)**	**Ultimate Load (kN)**	**Ultimate Load per Unit Length (N/mm)**	**Average Ultimate Load per Unit Length (N/mm)**
Nominal Length = 40mm				
a1	40.58	14.26	351	332
a2	40.20	13.00	323	
a3	40.53	13.03	321	
b1	40.23	13.25	329	315
b2	39.57	11.68	295	
b3	40.56	12.95	319	
Nominal Length = 60mm				
a1	60.42	18.22	302	302
a2	60.27	18.04	299	
a3	60.41	18.40	305	
b1	59.90	18.60	311	298
b2	60.11	17.83	297	
b3	60.57	17.38	287	

Comparison of Ultimate Tensile Strengths

The individual and average ultimate tensile strengths of the junctions have been calculated for the 40mm and 60mm long “a” and “b” groups of angle specimens. They

are given in Table 5. It is evident that that average ultimate tensile strengths of the junctions of the 76 x 6.4mm angle specimens are only similar when leg B is clamped, whereas the average ultimate tensile strengths of the junctions of the 76 x 9.5mm angle specimens are all very similar. Moreover, it appears that the average ultimate tensile strengths of the junctions of the thicker angle are about double that of the lowest strength of the thinner angle. However, they are significantly lower than the manufacturer's *minimum* transverse tensile strength [9] (see Table 1). In the case of the 76 x 6.4mm angle the lowest average ultimate tensile strength of the junction is little more than one-third of the latter value, whereas the average ultimate tensile strength of the junction of the 76 x 9.5mm angle is about two-thirds of the value.

Table 5

Comparison of ultimate tensile strengths of the junctions of 76 x 6.4mm and 76 x 9.5mm angles

Equal-Leg Angle Dimensions (mm)	**Nominal Length of Angle Specimen**	**Average Ultimate Tensile Strength of Junction (MPa)**	**Difference in Average Ultimate Tensile Strength (%)**
76 x 6.4	40[a]	30.5	77.6
	40[b]	17.2	
	60[a]	22.7	29.7
	60[b]	17.5	
76 x 9.5	40[a]	35.5	7.1
	40[b]	33.2	
	60[a]	32.3	3.0
	60[b]	31.4	

Note: [a] denotes leg A clamped, leg B in tension
[b] denotes leg B clamped, leg A in tension
Percentage difference = $[\{( )^a - ( )^b\}/( )^b] \times 100$

Comparison of Failure Modes of Angle-Leg Junctions

The failure modes of the twenty 40mm long 76 x 6.4mm angle specimens are shown in Figure 4.

(a) 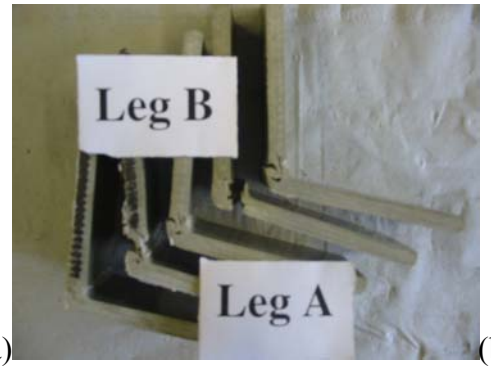

(b) 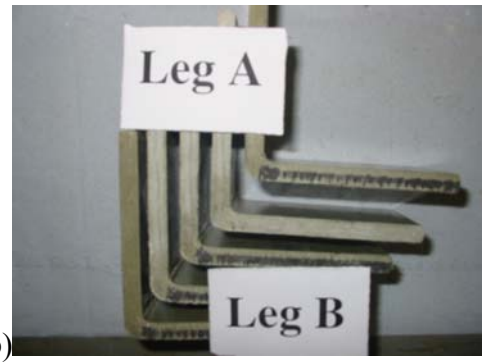

(c) 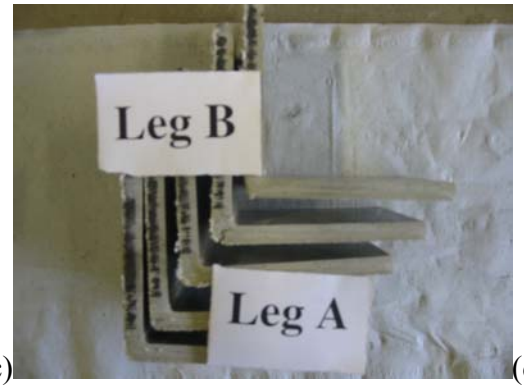

(d) 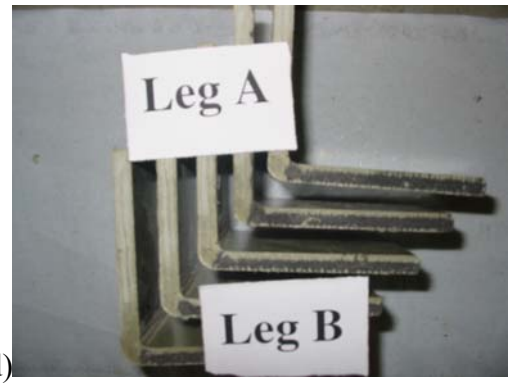

Figure 4: Failure modes of the 76 x 6.4mm equal-leg angles: (a) 40mm long specimens a1 – a5, (b) 40mm long specimens b1 – b5, (c) 60mm long specimens a1 – a5 and (d) 60mm long specimens b1 – b5.

It is clear from Figures 4(a) and 4(c) that there is much greater evidence of damage in the junction zone when leg A is clamped, whereas there is very little evidence of damage when leg B is clamped. Although only just about visible (see Figure 4(d)) in each angle specimen there is a crack running the length of the *instep*.

(a) 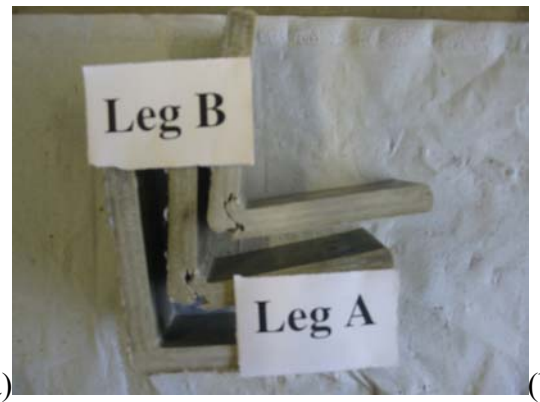

(b) 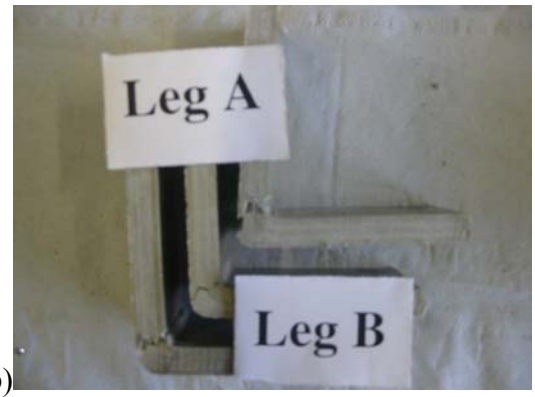

(c) 

(d) 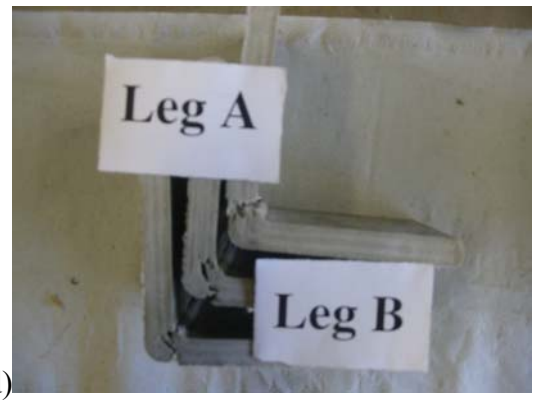

Figure 5: Failure modes of the 76 x 9.5mm equal-leg angles: (a) 40mm long specimens a1 – a3, (b) 40mm long specimens b1 – b3, (c) 60mm long specimens a1 – a3 and (d) 60mm long specimens b1 – b3.

Scrutiny of the junction failure modes of the 76 x 9.5mm angles depicted in Figure 5 reveals that they are very similar and this probably explains why the junction tensile strengths do not vary by more than about 7%. Moreover, in these angle specimens there is more evidence of uniformity of the fibre architecture around the junction than in the 76 x 6.4mm angle specimens.

CONCLUDING REMARKS

Tension tests were carried out on the leg junctions of thirty-two specimens cut from two thicknesses of pultruded GRP equal angle profile. The tensile strengths of the thicker (9.5 mm) angle specimens did not vary much irrespective of which leg was loaded in tension. On the other hand, the thinner (6.4 mm) angle specimens showed significant differences in strength depending on which leg (A or B) was loaded in tension. The strength differences of the thinner specimens were attributed to deviations from the ideal lay-up around the junction. The tests on the angle specimens showed that the tensile strengths of the angle-leg junctions ranged from about one-third to about two-thirds of the *minimum* transverse tensile strength of the angle-leg given in the manufacturer's design handbook [9].

ACKNOWLEDGEMENTS

The authors wish to thank the UK's Engineering and Physical Sciences Research Council (EPSRC) [Grant Ref.: GR/R28386/01] for supporting their research.

References

1. L.C. Bank and J. Yin, 'Analysis of progressive failure of the web-flange junction in post-buckled I-beams', *Journal of Composites for Construction* 3 4 (1999), 177-184.
2. D.W. Palmer, L.C. Bank and T.R. Gentry, 'Progressive tearing failure of pultruded composite box beams: experiment and simulation', *Composites Science and Technology*, 58 8 (1998), 1353-1359.
3. G.J. Turvey and Y. Zhang, 'A computational and experimental analysis of the buckling, postbuckling and initial failure of pultruded GRP columns', *Computers and Structures* 84 22-23 (2006), 1527-1537.
4. G.J. Turvey and Y. Zhang, 'Tearing failure of web-flange junctions in pultruded GRP profiles', *Composites Part A: Applied Science and Manufacturing*, 36 2 (2005), 309-317.
5. G.J. Turvey and Y. Zhang, 'Shear failure strength of web-flange junctions in pultruded GRP WF profiles', *International Journal of Construction and Building Materials*, 20 1-2 (2006), 81-89.
6. G.J. Turvey and Y. Zhang, 'Stiffness and strength of web-flange junctions of pultruded GRP sections', *Proceedings of the Institution of Civil Engineers: Structures and Buildings*, 158 SB6 (2005), 381-391.
7. G.J. Turvey and Y. Zhang, Characterisation of the rotational stiffness and strength of web-flange junctions of pultruded GRP WF-sections via web bending tests', *Composites Part A: Applied Science and Manufacturing*, 37 2 **(**2006), 152-164.

8. G.J. Turvey and Y-S. Zhang, 'Opening mode failure of pultruded GRP angle leg junctions'. In *Proceedings of the 3rd International Conference on Advanced Composites in Construction (ACIC 07)*, A.P. Darby and T.J. Ibell (eds.), 2nd – 4th April 2007, University of Bath, 389-393.
9. Anon., 'EXTREN fibreglass structural shapes: design manual', Strongwell, Bristol, Virginia, 1989.